



UNIVERSITÀ DEGLI STUDI DI TORINO

This is an author version of the contribution published on:

Questa è la versione dell'autore dell'opera:

*Contrasting environmental memories in relict soils on different parent rocks in the
south-western Italian Alps*

Quaternary International, xxx (2015) 1-14, 10.1016/j.quaint.2015.10.061

The definitive version is available at:

La versione definitiva è disponibile alla URL:

[<http://dx.doi.org/10.1016/j.quaint.2015.10.061>]

1 **Contrasting environmental memories in relict soils on different parent rocks in the South-**
2 **western Italian Alps**

3 Michele E. D'Amico*^{1,2}, Marcella Catoni¹, Fabio Terribile³, Ermanno Zanini^{1,2}, Eleonora Bonifacio¹

4 ¹Università degli Studi di Torino, DISAFA, Via Leonardo da Vinci 44, 10095 Grugliasco (To),
5 Italy.

6 ²Università degli Studi di Torino, NATRISK, Via Leonardo da Vinci 44, 10095 Grugliasco (To),
7 Italy.

8 ³Università degli Studi di Napoli Federico II, Facoltà di Agraria, Via Università 100, 80055 Portici
9 (Na), Italy.

10 *corresponding author: ecomike77@gmail.com

11

12 **Abstract**

13 Soils on the Alps are usually weakly developed, both because of the extensive Pleistocene
14 glaciations, and because of slope steepness and climate enhancing erosion. However, on some
15 stable, relict surfaces, particularly in the outermost sections of the Alpine range, some highly
16 developed soils are apparently in contrast with Holocene soil forming conditions. In this work we
17 wanted to assess the extent of pedogenesis in some of these soils, located under montane-level
18 vegetation in the Ligurian Alps (SW Piemonte, Italy), and relate it to the effects of climate and
19 parent material.

20 The considered well developed profiles showed signs of extremely different pedogenetic processes
21 on the different lithotypes. In particular, podzols with extremely thick E horizons (up to more than 2
22 m thick) and very hard, thick ortstein or placic horizons were formed on quartzite. Reddish "terra
23 rossa" Luvisols were formed on limestone. Red, extremely acidic Alisols were formed on shales.

24 The chemical properties, the micromorphology and the clay mineralogy demonstrated high intensity
25 pedogenic trends, and were characteristic of processes usually occurring under different climates.

26 They may therefore represent excellent pedo-signatures of different specific past

27 climatic/environmental conditions, as a response of different lithologies to specific soil-forming
28 environments, which range from warm and humid climates typical of red Alisols and Luvisols, to
29 cool and humid/wet climates leading to the formation of Podzols with ortstein/placic horizons.

30

31 **Keywords:** Alps; paleoenvironmental indicators; pedogenic processes; relict podzols; terra rossa
32 soils

33

34 **1 Introduction**

35 Soils in mid-latitude mountain areas are usually weakly developed (Legros, 1992) because of
36 geomorphic processes associated with active orogenesis and steep slopes, such as erosion and
37 deposition, and Pleistocene glaciations which erased most of the pre-existing soils. In fact,
38 normally, pedogenesis in these environments lasted for less than ca. 12000-16000 years (e.g. Egli et
39 al., 2006). Due to these constraints, only pedogenic processes associated with organic matter
40 dynamics reach a steady state and allow the development of Podzols or soils with Umbric/Mollic
41 horizons. These latter are known to form in less than 1000 years (Sauer, 2010), while Podzols may
42 develop in 500-3000 years under subalpine environments on the Alps (Egli et al., 2006; D'Amico et
43 al., 2014), although, if favorable conditions are maintained, the cheluviation phase may proceed
44 further and deepen the E horizons at the expenses of illuvial ones (McKeague et al., 1983). Intense
45 mineral transformations normally occur in longer periods and reflect climatic conditions. In
46 Mediterranean climates, well developed Bt horizons formed by clay lessivage are observed in early
47 Holocene or late Pleistocene soils (Sauer, 2010), while they can be observed in younger soils in
48 colder and wetter conditions (Sauer et al., 2009). Rubification, linked to abundant hematite
49 crystallization, is another slow process involving mineral weathering, and it is one of the most
50 widely used indicators of specific environmental conditions: it becomes visible only in soils older
51 than 100,000 years (Sauer, 2010).

52 Given the long time spans necessary for their formation, strongly weathered soils are very rare in
53 mid-latitude mountain ranges, where they can be preserved only on scattered stable surfaces located
54 outside the limits of Pleistocene glaciations (relict surfaces) and represent paleosols (when buried)
55 or relict soils (Ruellan, 1971). Both paleosols and relict soils keep traces of pedogenic processes
56 that have operated in the past and have been preserved for a long time, but in the case of relict soils
57 more recent processes are superimposed and polygenesis is the rule. The interpretation of soil
58 features as paleoenvironmental proxies should take into account therefore the most persistent
59 characteristics. Normally, the persistence of a soil property is inversely associated with its facility of
60 formation. Yaalon (1971) and, more recently, Targulian and Krasilnikov (2007) grouped soil
61 properties and horizons according to the time required for the attainment of a dynamic steady state
62 and, hence, their relative persistence: they can be rapidly adjusting and easily altered (developed in
63 less than 10^3 years), such as mollic and salic horizons and mottles, and slowly adjusting or
64 relatively persistent, as in the case of cambic, umbric, spodic and calcic horizons. Due to the very
65 long time needed for formation, oxic, albic, placic, argillic, petrocalcic, fragic and natric horizons
66 are considered very resistant to alteration. However, different pedogenic processes act on soils
67 during different periods of their existence, thus different properties superimpose in the same soil

68 horizons, creating a complex "combinations of older and newer records" (Targulian and
69 Goryachkin, 2004), and complicating the possible paleoenvironmental interpretations.
70 In this paper we report the morphological, chemical, mineralogical and micromorphological
71 characteristics of some well developed soils found on relict surfaces in a non-glaciated Alpine
72 region. The aim was to assess the pedogenic processes that have occurred to distinguish inherited
73 pedofeatures and link the soils with present and past environmental conditions, with special
74 emphasis on the effect of the parent material. We focused on soils showing traces of two main
75 weathering trends: two profiles had morphological evidences of rubification, while three profiles
76 were podzolic.

77

78 **2 Regional setting and study area**

79 Pleistocene glaciers occupied only small and scattered cirques above 1700-2000 m a.s.l. in the
80 Ligurian Alps (Piemonte, NW Italy) (Vanossi, 1990; Carraro and Giardino, 2004). The
81 geomorphology is therefore dominated by long term tectonic uplift, temporary peneplanation or
82 cryoplanation, followed by river incision, and periglaciation during cold Pleistocene periods. All the
83 geomorphic features derived from these processes are particularly well preserved in the Upper
84 Tanaro Valley (Fig. 1), where a series of relict surfaces (uplifted bedrock valley floor remnants) are
85 easily recognizable as flat summits and plateaus perched high above the valley floor, at different
86 altitudes on the north and south slopes because of differential tectonic uplift. On the south slopes,
87 many relict surfaces are located at different altitudes, possibly associated with different periods of
88 formation, while on the north slope all the surfaces are located at more or less the same level, gently
89 dipping from ca. 1600 m to 900 m a.s.l. following the valley downstream. On these gently sloping
90 plateaus and erosion terraces, erosion and deposition processes are very limited. Thus, they are
91 generally characterized by single rock substrates, without any significant colluvial/alluvial cover
92 layers. Morphologic indicators of relict preglacial or Early Quaternary surfaces (Goodfellow, 2007),
93 such as thick saprolite layers, blockfields and tors derived from in situ weathering and frost
94 shattering of the bedrock, are widespread on many of the considered surfaces and on the nearby
95 slopes. A precise chronology of the geomorphic events leading to the formation of the relict
96 surfaces is missing, but in other portions of the Ligurian Alps, some 50 km east from our study area,
97 remnants of analogous relict surfaces perched some hundreds of meters above the valley floors are
98 considered fragments of Pliocene alluvial terraces (Rellini et al., 2014).
99 We described and sampled in detail 5 well developed soil profiles on some of the relict surfaces
100 preserved in the Upper Tanaro Valley, chosen amidst a much larger number of observations
101 because of their good state of preservation and high degree of pedogenic development, in

102 topographic positions where visible disturbances due to erosion and deposition were minimal. The
103 main environmental properties of the sampling sites are shown in Table 1. A wide range of different
104 rock types were observed, ranging from sandy-textured quartzite (ALB soil, on "Quarzite di Ponte
105 di Nava"), to coarse quartzitic conglomerate (PLC soil, on "Porfiroidi di Melogno"), to quartzite-
106 andesite conglomerate (ORT soil, on "Porfidi di Osiglia"), to Fe-chlorite rich shales (ALI soil, on
107 "Formazione di Murialdo - Scisti di Viola"), to dolomite (TR soil, on "Dolomie di San Pietro dei
108 Monti") (Vanossi, 1990). The soil parent material was always the residuum formed from in situ
109 disintegration of the bedrock (regolith and saprolite). On quartzitic rocks, the unweathered substrate
110 appeared only as residual tors on the edges of the relict surfaces, otherwise thick layers of saprolite
111 (up to 20-50 m), which locally included some corestones (blocks of unweathered rock) represented
112 the parent materials for these soils.

113 Present day land use is montane *Castanea sativa* Mill., *Fagus sylvatica* L., *Ostrya carpinifolia*
114 Scop., *Pinus sylvestris* L. or *Pinus uncinata* Mill. forest (Table 1). The average annual temperature
115 ranges between 4° and 8°C, decreasing with altitude and with local variability with slope aspect.
116 The annual precipitation is around 800-1200 mm, with spring and fall maxima and summer minima
117 (Biancotti et al., 1998). Normally, water scarcity is not a limiting factor for plant growth (udic
118 moisture regime), even during the rather dry summer months (average July rainfall is around 40
119 mm). Summer fogs are common, thanks to the proximity with the Mediterranean Sea, and increase
120 available moisture in the surface soil layers. Snow cover normally lasts from November to
121 March/April in the considered altitudinal range, but snow thickness does not reach very high values
122 because of frequent winter rain episodes associated with warm Mediterranean air masses.

123

124 **3 Methods**

125 At the selected sites pits were opened and the soil profile described according to the FAO guidelines
126 (2006). In this work, we used qualifiers in brackets in horizon designation to indicate minor but
127 detectable characteristics. The soil samples were taken from the whole thickness of the genetic
128 horizons, air dried, sieved to 2 mm and analyzed. When not otherwise specified, the analyses
129 followed the methods reported by Van Reeuwijk (2002). The pH was determined potentiometrically
130 in water extracts (1:2.5 w/w). The total C concentration was measured by dry combustion with an
131 elemental analyzer (CE Instruments NA2100, Rodano, Italy). The carbonate content was calculated
132 by volumetric analysis of the carbon dioxide liberated by a 6 M HCl solution. The organic carbon
133 (OC) was then calculated as the difference between total C measured by dry combustion and
134 carbonate-C. The particle size distribution was determined by the pipette method after treating the
135 samples with H₂O₂ and dispersing with Na-hexametaphosphate. Exchangeable Ca, Mg, K, Na were

136 determined after exchange with NH_4 -acetate at pH 7.0. Acid ammonium oxalate and Na-dithionite-
137 citrate-bicarbonate were used to extract Fe and Al (Fe_o , Al_o , Fe_d and Al_d). The total element
138 concentrations (Al_t , Si_t , Fe_t , etc) were determined after HF- HNO_3 hot acid digestion (Bernas, 1968).
139 In all extracts, the elements were determined by Atomic Absorption Spectrophotometry (AAS,
140 Perkin Elmer, Analyst 400, Waltham, MA, USA). The presence of poorly crystalline allophane or
141 imogolite-type materials was assessed by pH measured in 1M NaF solution.
142 The mineralogical investigations were carried out using a Philips PW1710 X-ray diffractometer
143 (40kV and 20 mA, $\text{CoK}\alpha$ radiation, graphite monochromator). The mineralogy of the parent
144 materials was evaluated ($3\text{-}80^\circ 2\theta$) on backfilled, randomly oriented powder mounts. The Mg
145 saturated clay fraction ($< 2 \mu\text{m}$) was separated by sedimentation, flocculated with MgCl_2 , washed
146 until free of Cl^- , and freeze-dried. Scans were made from 3 to $35^\circ 2\theta$ at a speed of $1^\circ 2\theta \text{ min}^{-1}$, on air
147 dried (AD), ethylene glycol solvated (EG), and heated (550°C) oriented mounts. The presence of
148 hydroxyl-interlayered vermiculite (HIV) and/or hydroxyl-interlayered smectites (HIS) was
149 ascertained, and their thermo-stability assessed, by heating the samples to 110, 330 and 550°C .
150 Crystalline Fe and Al oxi-hydroxides were detected on backfilled, randomly oriented mounts of the
151 separated clay fraction ($5\text{-}40^\circ 2\theta$), at a speed of $0.5^\circ 2\theta \text{ min}^{-1}$.
152 Oriented and undisturbed bulk soil samples or aggregates were collected from the profiles and
153 impregnated with resin to prepare 60×45 mm thin sections. The thin sections were observed using a
154 polarizing microscope (Leitz Wetzlar HM-POL) and described following Stoops (2003).
155 Hue, chroma and value of the Munsell notation were used to calculate the redness rating following
156 the procedure described by Torrent et al. (1980).
157 The set of analyses performed was selected depending on the type of soil and horizon to be studied.

158

159 **4 Results**

160 **4.1 ALB: Morphology, chemistry and clay mineralogy**

161 ALB developed on sand-grained quartzite; the XRD and total elemental analysis of the parent
162 material confirmed that the sandy-textured, weakly metamorphosed quartzite was mainly composed
163 of quartz, with only traces of micas and feldspars. On this substrate, on flat topography, soils had
164 extremely thick E horizons (more than 2.1 m, Table 2). Only the top 35 cm (AE horizons) likely
165 developed in a periglacial cover bed, evidenced by a few weakly weathered cobbles, separated from
166 the 2EA and 2E horizons below by a sharp discontinuity which included some thin soil wedge cast-
167 like structures (Fig. 2A). Below the periglacial cover bed, the thick E horizons were composed of
168 strongly weathered, white-greyish quartzitic coarse sand locally impregnated by percolated organic
169 matter and abundant fungal hyphae associated with the pine deep root system. Two Bs horizons,

170 with different morphologies, were collected nearby. The first one (Bs-old in Tables 2, 3 and 4) was
171 observed ca. 30 m south-east of the main profile, below a fallen tree on a slightly steeper, recently
172 eroded surface. Below a thinner E horizon, very similar to the deep E in the main profile, the upper
173 limit of the Bs was wavy and irregular, and its pale yellowish-brown material was interrupted by
174 many whitish/greyish spots. This Bs horizon was much paler than those developed on the steep
175 surfaces around (Bs-young in Tables 2, 3 and 4).

176 The 2E horizon had the smallest textural clay content (Table 3) and was the most depleted in total
177 and oxalate extractable metals (Table 4). In the Bs-old horizon the concentration of extractable Fe_o
178 and Al_o was much lower than in the Bs-young (SI, i.e. spodic index: $Al_o + 0.5Fe_o$, 0.23% and 0.84%,
179 respectively, Table 4), as well as the pH_{NaF} (9 and 12.5, respectively, Table 3), indicating a smaller
180 amount of short range-ordered materials, such as imogolite, proto-imogolite and allophane.

181 In the E horizon, the shift of the 1.4 nm peak and of the broad one around 1.2 nm to, respectively,
182 1.63 and 1.3-1.4 nm after EG solvation evidenced that clay was dominated by smectites and
183 smectite-illite mixed layered minerals. Illite and quartz, inherited from the parent material, were
184 detected as well. A good collapse upon heating was observed and indicated the absence of Al
185 polymers in the interlayer (Fig. 3A).

186 Smectitic minerals were detected in the clay fraction of the Bs-old as well, associated with
187 interstratified minerals, such as illite and non-swelling components. Even after heating at 550°C,
188 the peak at 1.0 nm was asymmetrical, indicating the presence of HIV (Fig. 3A).

189

190 **4.2 ORT: soil morphology, chemistry, clay minerals and micromorphology**

191 The weakly metamorphic quartzitic conglomerates with andesitic inclusions, parent material of
192 ORT soil, included small quantities of mafic minerals, such as pyroxenes and amphiboles, in
193 addition to quartz (still the most important mineral by far), micas and feldspars. It was slightly Fe
194 and Al-richer than the parent material of the ALB soil (section 4.1). The thick saprolite layer was
195 depleted in mafic minerals compared to the unweathered rock, but without detectable amounts of
196 any pedogenic materials.

197 Although the eluvial horizon of ORT was thinner than that observed in ALB, it still showed a
198 remarkable development of cumulatively ca. 140 cm (Fig. 2B). The albic horizons were followed
199 by a thick and strongly cemented sequence of ortstein horizons (Table 2). The upper loose,
200 bioturbated E horizon was probably developed in a periglacial cover bed, as shown by sharp
201 variation in structure and consistence, by the higher stone content and the much weaker weathering
202 degree of the stone fraction. Below, the 2Ex and 2E(h) had a hard consistence, almost cemented in
203 the field, and showed many darker patches distributed on net-like structures, apparently enriched in

204 illuvial organic matter. Though these horizons cannot be considered true fragipans, the net-like
205 appearance and the quick slacking of hard dry aggregates in water evidenced fragic properties.
206 Below, a thin 2Btm(s) horizon was observed, characterized by reddish clay coatings on the upper
207 faces of cemented peds. The 2Bsm horizon was a typical ortstein, strongly cemented and with
208 abundant macroporosity, as often observed in ortstein horizons on the Alps (e.g., Catoni et al.,
209 2014). Also the thick deeper 2Btsm horizon was characterized by strong cementation, but it showed
210 thick reddish illuvial clay coatings on the upper faces of peds. Both 2Btsm and 2Btm(s) horizons
211 showed an increase in clay content compared to the nearby E and Bsm ones (Table 3). The bottom
212 yellowish brown 2Bsh_m was darker than the horizons above, likely because of decay of present-day
213 roots, which were concentrated in the fissures between cemented, coarse aggregates. Between the
214 2Bsh_m and the hard, unweathered rock, a pale and weakly cemented C_m and a strongly weathered
215 saprolitic C_r horizons were visible along a nearby roadcut.

216 The micromorphology of E and Bsm/Btm horizons confirmed many of the macromorphological
217 features observed in the field (Table 5). The groundmass of the two thick E horizons was
218 characterized by a close porphyric coarse/fine (c/f) related distribution pattern, with few coarse
219 vughs or cracks (Fig. 4A, 4B). Some cracks were partially filled with rounded silty quartz grains
220 and thin monomorphic organic matter infillings; these cracks were cut both through the fine matrix
221 and the shuttered coarse fragments. Silt infillings and oriented fine sand/silt caps were common.
222 The groundmass was locally thinly laminated. A few reddish clay coatings and pedorelicts were
223 locally observed in the 2Ex, while the white groundmass was locally slightly darker because of
224 organic matter or redoximorphic Fe-Mn impregnations.

225 The 2Bsm horizon had a high porosity (Table 5, Fig. 4C), which separated strongly developed
226 subangular blocky peds characterized by a closed porphyric c/f related distribution (Fig. 4C). Many
227 reddish or yellowish brown clayey pedorelicts were observed in the groundmass. Locally, disrupted
228 reddish clay coatings were preserved on the void walls, surmounted by thinly laminated silt and fine
229 sand accumulations. In turn, these accumulations were covered by thick, composite, cracked
230 yellowish-brown coatings, characterized by at least 3 paler or darker layers. Both the groundmass
231 and the silt accumulation were impregnated by yellowish-brown amorphous materials. These
232 amorphous coatings represented almost 13% of the total solid volume, in agreement with the high
233 Fe_t and Al_t measured in this horizon (Table 4).

234 The micromorphology of the 2Btsm below was distinctly different (Table 5, Fig. 4D). In particular,
235 a banded distribution of differently sized particles was observed, usually associated with varying c/f
236 related distribution patterns (Fig. 4D). Closely packed layers with porphyric related distribution,
237 where small or medium angular quartz grains were included in a fine matrix impregnated by black

238 and dark reddish-brown materials, were in continuity with layers composed of thick, thinly
239 laminated silt accumulations covered by thick crescentic clay coatings and infillings. These layers
240 rich in illuvial clay were in continuity with loose layers with chitonic related distribution and
241 abundant compound packing voids, where coarse angular quartz fragments were surrounded by
242 cracked yellowish-brown coatings probably consisting of Fe-Al oxi-hydroxides and monomorphic
243 organic matter.

244 Despite the clear podzolic morphology, low amounts of Fe_o and Al_o were measured (Table 4), and
245 the SI never reached the 0.5%, required by most taxonomic systems in the spodic horizon
246 definition. Particularly low values of poorly crystalline Fe-Al (hydr)oxides were measured in the
247 top 2Btm(s) and a low Fe_o/Fe_d ratio was measured in the other illuvial horizons as well; only the
248 deep 2Bshm had a high proportion of poorly crystalline Fe oxides. The pH_{NaF} had low values in the
249 2E(x) and in the 2Btm(s) horizons, and reached the highest values (11.0 and 11.8 respectively) in
250 the 2Bsm and in the 2Bshm. Abundant short range-ordered imogolite-type minerals thus
251 characterized these horizons. The many-fold increase of Fe_t and Al_t from the E to the ortstein
252 horizons indicated a strong redistribution of these metals, but an irregular trend in the different
253 2Bsm and 2Btsm (Table 4). In the illuvial horizons, more than 40-50% of total Fe was in the form
254 of pedogenic oxides, with the exception of the 2Bsm, which showed a low Fe_d/Fe_t .
255 In spite of the unusual distribution of metal forms along the profile, clay mineralogy was consistent
256 with that typically characterizing Podzols. E horizons contained smectites, illite-smectite, and traces
257 of chlorite-vermiculite interlayered minerals (Fig. 3B). The clay mineralogy of the illuvial 2Bsm
258 and 2Btsm horizons was similar to each other. Small traces of swelling minerals were evidenced by
259 the appearance of a small peak at 1.64 nm after EG solvation only in the top 2Btm(s) horizon, while
260 the most abundant minerals were illite, mixed layer minerals with an illitic component and HIV.
261 Some chlorite seemed also to be present, since a small peak at 0.7 nm remained after heating at
262 550°C. Kaolinite (double peak near 0.72 nm completely collapsing at 550°C) was detected as well.
263 Quite large amounts of gibbsite (peaks at 0.48 nm) were observed in the 2Bsm and in the 2Btsm
264 horizons. Only quartz and primary chlorites and micas were detected in the saprolitic Cm and Cr
265 horizons; here, the mafic minerals included in the unweathered rock were not detected.

266

267 **4.3 PLC: Morphology, micromorphology, chemistry and clay minerals**

268 PLC was sampled on hard and coarse metamorphic quartzitic conglomerates, which included the
269 same primary minerals of quartzite (see section 4.1), but with a larger muscovite content. On gentle
270 slopes near the surface edges, placic horizons were common and well developed between the E
271 horizons and the underlying cemented ortstein ones. These soils had thinner (ca. 70 cm) E horizons;

272 the deep E horizon (2E(x)) had a very similar macro-morphology compared to the ones observed in
273 the ORT (section 4.2.2), with hard consistence and weak fragic properties (Table 2, Fig. 2C).
274 Despite the hard consistence, the 2E(x) horizons in thin section had a rather high void content
275 (Table 5, Fig. 4E). The c/f related distribution of the aggregates was open porphyric, with a dense
276 silt and fine sand matrix surrounding angular to subrounded sand grains, and larger gravel-sized
277 clasts. The matrix was thinly laminated and convoluted and it was locally impregnated with
278 monomorphic organic matter. Well developed silt caps and compression caps were visible close to
279 the coarse fragments (Fig. 4E). A few pores had reddish-brown clayey infillings, while a few
280 reddish pedorelicts were included in the matrix. The placic horizon had a double-spaced to open
281 porphyric c/f related distribution (Fig. 4F): coarse and fine quartz grains, subangular in shape, with
282 few weakly weathered feldspars and strongly weathered phyllosilicates were included in a dark
283 reddish matrix with black bands (as normal in placic horizons, Wilson and Righi, 2010). The black
284 bands were convoluted. A very low porosity was detected. Below, the placic horizon graded into the
285 2Bsm2, characterized by a higher porosity (compound packing voids) and a geric c/f related
286 distribution. The matrix was impregnated by yellowish-brown materials, which covered the pore
287 walls as compound cracked coatings, characteristic of spodic horizons. Above the placic horizon,
288 dense and layered fine sand accumulations were developed.

289 Despite the hard cementation of the placic and ortstein horizons, only small quantities of Fe_o and
290 Al_o were detected (Table 4), likely because of the quartzitic coarse sand matrix diluting the illuvial
291 spodic materials. However, the high Fe_o/Fe_d ratio indicated that Fe illuviation is still active. Al_o was
292 not significantly translocated to these cemented horizons, while the Fe_o increased 15 times from the
293 Fe-depleted E to the cemented 2Bsm1 and 2Bsm2.

294 Lepidocrocite was detected by XRD (evidenced by the sharp 0.63 nm peak) in the cemented Bsm
295 horizons, and it was most abundant in the placic Bsm1 (Fig. 3B). As normal in Podzols, smectite
296 and illite-smectite interlayered minerals were abundant in the clay fraction of E horizons, while
297 illite, HIVs and chlorites were dominant in the underlying placic and ortstein horizons.

298

299 **4.4 TR: Soil morphology, chemistry and clay mineralogy**

300 The dolostone, parent material of TR, was composed of pure dolomite but included some thin marly
301 veins with micas, chlorites, feldspars and quartz. Upslope from this profile, Fe-chlorite rich shales
302 outcropped. On this dolostone, soils were typical Mediterranean "terra rossa", with hue of 2.5YR in
303 all B horizons (Table 2). On the quarry scarp where the samples were collected, the thickness of
304 these red soils varied from 50 cm to more than 5 m, filling cracks and hidden sinkholes.

305 A very high clay content (up to 73% in the Bt1), abundant and thick clay coatings on the ped
306 surfaces and near-neutral pH values characterized these soils (Table 3). The ratio between CEC and
307 clay may be as low as 0.27 in the Bt1 horizon (Table 3) where the highest decrease in the Si_t/Al_t
308 molar ratio was also visible: it passed from 2.0 in the Cr layer to 1.8 (Table 4). In all horizons,
309 pedogenic Fe oxides were abundant and the Fe_o/Fe_d ratio indicated a high crystallinity of Fe forms.
310 The calculated redness rating of 15 lied within the range found in Spanish pre-Riss (MIS 11 and
311 older) Luvisols where it corresponded to hematite contents of about 2% (Torrent et al., 1980). As
312 the molar weight of hematite is 160, around 14 g kg^{-1} of Fe_d should originate from 2% of hematite.
313 The Fe_d amounts of 43-45 g kg^{-1} (Table 4) suggested therefore that pedogenic Fe forms in Bt
314 horizons consisted of a 1:2 mixture of hematite and goethite (molar weight=89). As hematite is
315 highly pigmenting, particularly in Mediterranean soils (Torrent et al., 1983) even small amounts
316 may give the soil the red and bright colour (2.5YR 4/8 in the Bt horizons).
317 The clay fraction was a mixture of regularly interstratified swelling minerals, as visible from the
318 partial shift of the 1.4 nm peak to 1.55 nm upon EG solvation and the concomitant shift of the 2.83
319 nm peak, some chlorite, vermiculite, illite and kaolinite (Fig. 5). Although not present any more in
320 the clay fraction, dolomite was still visible in the powdered bulk samples, thus favouring a high Ca
321 and Mg concentration in the soil solution and the consequent high base saturation.

322

323 **4.5 ALI: Soil morphology, chemistry and mineralogy**

324 ALI developed on shales, which were composed by Fe-rich chlorites, muscovite, biotite, quartz, and
325 smaller quantities of feldspars, amphiboles and margarite.

326 Very red colours (2.5YR 4/6 or 2.5YR 5/8 in the Bt horizons) characterized also highly weathered,
327 extremely acidic and desaturated Alisols (Table 2, Fig. 2E). These soils had well-expressed argic
328 horizons, with more than 50% of clay and common clay coatings and Mn coatings, covering the
329 faces of well-expressed angular peds (Tables 2 and 3).

330 Also in this case, large amounts of Fe_t (50-60 g kg^{-1} , Table 4) were found in the Bt horizons. The
331 redness rating (11.25) was slightly lower than that of the TR soil (section 4.4), suggesting a
332 hematite content of about 15 g kg^{-1} (Torrent et al., 1980). On average, the Fe_d content in the Bt
333 horizons was 36 g kg^{-1} , thus the ratio between hematite and goethite should be around 1:2.6. The
334 ratio CEC/clay was always above 50 and also in this case, a slight depletion of Si with respect to Al
335 was visible from the changes in Si_t/Al_t molar ratio (from 2.24 in the parent rock to 2.16 in the 2Bt2).
336 XRD analysis of powder samples from the most weathered and least disturbed 2Bt2 horizon
337 confirmed a strong mineral weathering, evidenced by the differences with the parent material. The
338 ratios between the 1.4 nm peak of chlorite and the 4.26 of quartz changed from 2.1 in the parent

339 material to 0.7 in the 2Bt2 horizon, indicating a strong depletion of chlorite compared to quartz.
340 Micas were depleted as well, with ratios passing from 3.0 to 0.7. Furthermore, lithogenic chlorite
341 was probably completely degraded as no peaks at 1.4 or 0.7 nm were found after heating to 550°C.
342 The collapse of the 1.4 nm phase started at 330°C and at 550° only a broad diffraction peak at 1.2
343 nm was visible (Fig. 5). This behaviour suggests the presence of a mixed layer component made by
344 HIV with a high degree of Al-polymerization together with a more resistant 1.4 nm phase
345 (Tolpeshta et al., 2010). Kaolinite and traces of smectite were present as well.

346

347 **5 Discussion**

348 **5.1 Pedogenic processes in strongly developed podzolic soils**

349 On quartzitic materials, podzolization has apparently been active for extremely long periods, as
350 shown by the extreme development of E horizons (in the ALB and ORT soil) or the strong
351 cementation of thick ortstein layers (ORT soils). Soils of probable Holocene age, formed on nearby
352 steeper slopes on the same parent materials, are Podzols with 20-40 cm thick E horizons and thin
353 weakly cemented layers. Extremely thick E horizons have sometimes been observed in tropical
354 Podzols (e.g., Dubroeuq and Volkoff, 1998), created during long periods of pedogenesis associated
355 with warm and wet climate. At mid and high latitudes, E horizons are usually thinner also in ancient
356 soils developed on permeable sandy materials on stable marine terraces: for example, the extremely
357 impoverished and ancient Podzols (more than 500,000 years old) developed below the pygmy forest
358 in California on Pleistocene sandy beach deposits have ca. 30-40 cm thick E horizons (Jenny et al.,
359 1969).

360 Despite the strong features left by long lasting podzolization, normally associated with cool and
361 humid climates and acidifying coniferous forests and/or ericaceous shrubs, many different
362 environmental memories are imprinted in these podzolic soils, pointing to an ancient polygenetic
363 origin as well (Tursina, 2009). Cryoturbation features (Cremaschi and Van Vliet-Lanoë, 1990; Van
364 Vliet-Lanoë, 2010), created during cold phases, were well preserved. In fact, we observed small
365 wedge cast-like figures at the contact between the cover bed and the in-situ E horizons in ALB, hard
366 consistence, silt accumulations, dense packing and other properties characterizing fragic horizons in
367 ORT, hard consistence, convoluted platy microstructure and abundant silt caps in PLC. All these
368 features suggest that more than one glacial period has elapsed since the beginning of soil formation.
369 We can assume that these cold phases correspond with Pleistocene glacial periods, as during the
370 coldest Holocene periods (i.e., the Little Ice Age, Joerin et al., 2006) the temperatures were only ca.
371 1°C lower than present day ones (Lühti, 2014); temperatures at least 4-7°C lower than present day
372 ones would be necessary for the development of large and thick solifluction and gelifluction

373 deposits (Harris, 1994) and these conditions were likely verified only during the coldest Pleistocene
374 climatic phases. Moreover, these landforms could not form under dense beech or pine forests,
375 which have covered the area throughout the Holocene (Ortu et al., 2008).

376 The 2Bsm and 2Bt_{sm} horizons in the ORT soil bring many other indicators of strong polygenesis,
377 each associated with different glacial and interglacial periods. In particular, in the 2Bsm, the reddish
378 clayey rounded pedorelicts included in the groundmass and the disrupted clay coatings around a few
379 voids are remnants of an ancient well developed Bt horizon, likely similar to the 2Bt_{sm} below. The
380 thick layered silt accumulations observed above the disrupted argillans were probably deposited
381 during periods of intense frost disturbances, which may have also destroyed the previously existing
382 clay coatings (Collins and O'Dubhain, 1980; Kemp, 1998). The most recent pedogenic features
383 seem to be the accumulation of thick amorphous yellowish-brown, cracked coatings, which are
384 characteristic of spodic horizons and are caused by the desiccation of the hydrated illuvial organic
385 matter associated with amorphous Al and Fe (Buurman and Jongmans, 2005). In the Bt_{sm} horizon,
386 layers of silt are deposited between thick reddish clay coatings, demonstrating different phases of
387 cryoturbation followed by warm and seasonally wet periods, during which the vegetation was
388 possibly converted from coniferous forest to other, less acidifying vegetation types. Also in this
389 horizon, the last phase seems dominated by the deposition of thin coatings of spodic materials in the
390 pore-rich, chitonic portions of the horizon. The superimposition of different Bsm and Bt_m horizons,
391 their very different c/f related distribution and the chemical composition might suggest the
392 existence of unnoticed lithological discontinuities associated with ancient periglacial cover beds,
393 which could improve the interpretation of the chronology of the different pedogenetic phases.

394 Memories of particularly humid environmental conditions are preserved in the PLC soil while they
395 were not detected in the ALB and PLC soils, because of topographic position and parent material
396 granulometry. Placic horizons are often found in hydromorphic soils, usually in humid oceanic or
397 montane tropical climates (e.g., Lapen and Wang, 1999; Jien et al., 2010), and they are uncommon
398 in Holocene soils on the Alps, where they have only been described in the much more humid north-
399 western French Alps (Thouvenin and Faivre, 1998). Placic horizons form upon the crystallization of
400 Fe/Mn oxi-hydroxides from dissolved divalent ions, triggered by changes in redox potential
401 (Bockheim, 2011), thus periodical waterlogging is essential. Lepidocrocite was detected in the
402 placic horizon, and in the underlying ortstein, confirming the shift in redox conditions. This mineral
403 is common in redoximorphic soils in many environmental conditions, but its stability is strongly
404 enhanced by the presence of complexing organic molecules (Krishnamurti and Huang, 1993) and by
405 dissolved Al (Schwertmann and Taylor; 1989, Chiang et al., 1999), and is thus well preserved in
406 periodically waterlogged podzolic soils, and in placic horizons (Campbell and Schwertmann, 1984).

407 On the other hand, the cementation of the ortstein horizon below the placic and the typically
408 cracked, yellowish-brown monomorphic coatings on the aggregate surfaces indicate that a strong
409 illuviation of organic Fe-Al complexes has been active, at least in some periods along the history of
410 this soil. Moreover, clay mineralogy, both in the E and in the ortstein horizons, has the normal
411 depth trend for podzolic soils, nonetheless the weak Al_0 redistribution with depth.

412 The PLC soil was therefore characterised by both podzolization and hydromorphism, and in these
413 cases, the horizons above the cemented layer tend to partially lose the spodic characteristics, which
414 are instead well maintained below the placic horizon (Bonifacio et al., 2006).

415 Waterlogging and related redox processes are unlikely active in present day climate, unless maybe
416 during periods of intense snow-melt in spring, but might have been common during wet Quaternary
417 phases, or when permafrost inhibited internal drainage in this soil, or when large quantities of water
418 were available during permafrost melting. These horizons, thus, bring memories of past, more
419 humid conditions which seem to have occurred after a first phase of intense podzolization and are
420 not imprinted in the other studied soils. PLC is thus another example of a highly polygenetic soil,
421 where podzolization associated with ortstein cementation, followed by waterlogging, placic horizon
422 formation and lepidocrocite crystallization acted during different periods, yet to be discovered.

423 Cryoturbation features such as laminated and convoluted microstructure and silt and compression
424 caps around coarse fragments in the 2E(x) horizon, suggest that also in this case more than one
425 Pleistocene glacial period has elapsed since the beginning of pedogenesis.

426 Other indicators of old age for the ALB, ORT and PLC soils are the high crystallinity of the Fe
427 oxides in the podzolic horizons (evidenced by the low Fe_o/Fe_d ratio) and the abundant gibbsite in
428 the ORT B horizons. Abundant gibbsite in soil horizons and saprolite layers has often been
429 associated with pedogenetic phases occurred during warm Early Pleistocene interglacials or during
430 the Tertiary (e.g., Mellor and Wilson, 1989). However, this assumption has sometimes been
431 challenged by other studies (e.g., Goodfellow et al., 2014), which state that gibbsite can form from
432 the early dissolution of Al-bearing feldspars in saprolitic layers also in cold and slightly acidic soil
433 environments, thus reducing the pedogenetic and paleoenvironmental significance of this mineral.

434 However, the saprolite at the ORT base did not include gibbsite, thus its abundance in the cemented
435 ortstein horizons could point to a crystallization from amorphous materials, following the
436 mineralization of the Al-complexed organic matter (Righi et al., 1999).

437 Despite the ancient origin, the podzolization process is still active in the considered soils. The E
438 horizons of all these ancient Podzols clearly bring evidence of percolation of soluble organic matter
439 and show the typical clay mineral associations of present-day podzolic E horizons, with abundant
440 smectites and smectite-interlayered minerals (Ross, 1980), derived from the transformation of micas

441 and chlorites to vermiculite (Wilson, 1999). Many Bs or Bts horizons are likely being depleted in Fe
442 and Al oxi-hydroxides and in imogolite-type materials because of the expansion of the E horizon at
443 depth. The Bs-old in the ALB soil shows a particularly advanced degradation, as indicated by the
444 suite of minerals in the clay fraction, that contains HIV, non-swelling mixed layers and smectite.
445 Smectitic minerals are seldom detected in the Bs horizons of Podzols (e.g., Righi et al., 1982;
446 Cornelis et al., 2014). It seems therefore that present-day conditions favour the removal of Al-
447 polymers from the interlayer in the Bs, which occur upon downwards migration of podzolic sequa
448 (Falsone et al., 2012). The light greyish or yellowish patches, and the wavy irregular upper limit of
449 the pale yellowish brown Bs-old horizon were likely related to zones with higher or lower porosity,
450 which favoured or inhibited water percolation and, thus, locally promoted chelation and depletion
451 of the accumulated spodic materials by soluble organic matter (as often observed in tropical
452 Podzols, Buurman et al., 1999). The 2Btm(s) in the ORT soil, which was impoverished in oxalate-
453 extractable elements and had some smectite in the clay fraction, evidences the same degradation
454 process, likely associated with a deepening of the E horizon.
455 Podzolic soils are characteristic on quartzitic parent materials in the study area, and variations in
456 specific properties depend mostly on parent material mineralogy and texture. In fact, the strong clay
457 illuviation detected in the ORT soil was possible because of the presence of small quantities of
458 weatherable mafic minerals which permitted the formation of a large amount of phyllosilicates. On
459 purer quartzite and quartzitic conglomerate, this clay formation and illuviation was not possible,
460 even under presumably similar climatic regimes.
461 The different topographic position could explain other variations in soil features: for example, the
462 coarser texture characterizing the PLC soil compared to the ALB and ORT can be associated with
463 the closeness to the edge of the relict cryoplanation surface that could have helped the selective
464 removal of fines, particularly during highly erosive cold periods. The strong waterlogging indicators
465 characterizing the PLC soil are widespread on similar surface morphologies on the same substrate
466 lithology in the non-glaciated Upper Tanaro Valley.

467

468 **5.2 Pedogenic processes in the rubified soils**

469 Terra Rossa soils are typical of the Mediterranean areas, but may occur also in axeric climatic
470 regimes (Boero and Schwertmann, 1989) if a highly permeable substrate, such as coarse limestone
471 glacial and alluvial deposits, enhance summer desiccation. Present-day climatic conditions in the
472 study area are quite far from the Mediterranean, as no warm and dry seasons occur (Biancotti et al.,
473 1998) or have occurred during the whole Holocene; in fact, despite the lack of precise rainfall
474 reconstructions, summer precipitations were abundant also during the warmest period (i.e., the

475 climatic optimum, ca. 8000-4000 years B.P.) as shown by the lack of Mediterranean or xerophilous
476 taxa in palynological records collected in nearby valleys (Ortu et al., 2008). Like many rubified
477 paleosols in non-Mediterranean areas, the TR soil has probably developed during previous
478 interglacials or even during the early Quaternary or Late Tertiary, when the climate was
479 characterized by warmer temperatures and a stronger rainfall seasonality (Busacca and Cremaschi,
480 1998). The distribution of Fe forms, in both the TR and the ALI soil, confirm the long time elapsed
481 since the beginning of pedogenesis and climatic changes during soil formation. A mixture of
482 hematite and goethite is typical of many Terra Rossa soils (e.g. Boero and Schwertmann, 1989;
483 Durn et al., 1999; Jordanova et al., 2013) and has been explained by the shift in climatic conditions
484 that, when hot and dry, favour the transformation of ferrihydrite into hematite, and when moister
485 promote ferrihydrite dissolution and goethite precipitation (Schwertmann and Taylor, 1989). In both
486 soils goethite dominated over hematite but the calcareous soil was slightly more hematite-rich. The
487 larger hematite content in TR may be related to the presence of a more compact and fractured
488 parent material that favours drainage of excess water even during the moistest periods.
489 The genesis of Terra Rossa soils is still a matter of debate as the insoluble residue of the calcareous
490 parent material has been shown to be insufficient in many cases to permit soil formation. Based on
491 mineralogy, rare earth elements, particle morphology and other indicators (Durn, 2003), colluvial
492 processes and aeolian dusts, mainly from Sahara, are thought to extensively contribute (Yaalon,
493 1997), as well as loess sediments from Middle Pleistocene (Durn et al., 1999). The mineralogy of
494 Saharan dust in the Western and Northern Mediterranean region is dominated by quartz, illite,
495 palygorskite, with minor amounts of smectites, feldspars and dolomite (Avila et al., 1997). With the
496 exception of palygorskite, unstable in non-aridic soils, all other minerals were found in the TR soil,
497 but being ubiquitous, may have many origins and most of the detected minerals in the bulk soil
498 were also present in the marly veins included in the substrate, and in nearby shale outcrops.
499 Moreover, despite the increase in TiO_2 contents from the Cr to the Bt horizons (i.e. from 0.1 to
500 0.8%, data not shown), the ratio between Al_t and Fe_t remained almost constant in all soil horizons,
501 suggesting an autochthonous origin. By assuming that Ti is not leached nor added to the soil during
502 pedogenesis and therefore its concentration in a soil horizon fully originated from the dissolution of
503 the parent material and depletion of other more mobile elements, we calculated the losses of all
504 element oxides following the approach illustrated by Krauskopf and Bird (1985). According to
505 these calculations, the weight loss when passing from the saprolite to the Bt horizons was around
506 80-82%, thus the dissolution of 1 kg of saprolite may have originated 180-200 g soil. Although
507 higher than the average insoluble residue reported for the parent material of Terra Rossa soils in
508 Mediterranean environment (Yaalon, 1997), these data are compatible with the presence of the

509 marly veins. Assuming an average dissolution rate of $40 \mu\text{m y}^{-1}$ (i.e. the maximum of the range
510 reported by Yaalon, 1997) and a content of insoluble residue of 20%, no much less than 700,000
511 years would have been necessary to form the 5 m soil thickness locally observed on the quarry
512 scarp. Considering that limestone dissolution was probably much slower during cold and dry glacial
513 periods (as hypothesized by Priori et al., 2008), the time frame could become even longer.
514 Both TR and ALI soils keep traces of previous warm, seasonally dry environments, but it is the
515 difference in parent materials that mainly differentiate present-day properties. The dissolution of
516 carbonatic rocks in TR maintained a high Ca and Mg concentration and a high pH that favoured the
517 stability of smectite (Wilson, 1999), while in the ALI soil, on Fe-rich chloritic shales, only traces of
518 swelling minerals were found. Despite the presence of smectite, the clay CEC was rather low in
519 both soils, although slightly higher in ALI than in the TR, in agreement with the trend in Si losses
520 during soil formation. The solubility of Si is almost independent from pH below pH 8.5 (Drees et
521 al., 1989), a pH value that is not reached in the presence of calcite, but may be overcome when the
522 more soluble dolomite is present (Bloom, 2000). Dolomite may have therefore induced a higher Si
523 depletion, favouring the stability of kaolinite in the TR soil, while the acidic environment of the
524 chloritic shales caused lower Si losses and favoured Al mobilization and precipitation in the
525 phyllosilicate interlayer. As kaolinite was abundant also in ALI Bt horizons, the higher CEC/clay
526 ratio is likely also related to a decrease in the stability of the Al polymers in the HIV at the acid pH
527 of the present day Bt horizons.
528 Thus, these two hematite-rich soils likely formed under subtropical conditions in some ancient
529 times. The strong mineralogical weathering and the geochemical data are memories of periods
530 characterized by hot subtropical or Mediterranean climates, which have very different weathering
531 and pedogenic regimes compared to present day conditions. In fact, Rellini et al. (2014) state that
532 kaolinite and hematite formation probably occurred during ancient pedogenetic phases, during the
533 late Pliocene or the early Pleistocene in the Ligurian Alps.

534

535 **5.3 Environmental memories and soil processes**

536 Large areas of the upper Tanaro Valley were never glaciated, and many relict surfaces are preserved
537 on its slopes. Many geomorphic indicators (tors, blockfields, thick saprolite layers, etc.),
538 particularly well preserved on hard quartzitic substrates, are often considered to be originated before
539 the Quaternary, or at least in the early Quaternary (Migoñ and Lidmar Bergström, 2001;
540 Boelhowers, 2004; Goodfellow, 2007) and confirm that the considered relict surfaces are actually
541 ancient. Moreover, the high clay content (up to more than 20% clay) characterizing saprolite and
542 soil layers on hard quartzitic rocks, extremely poor in phyllosilicates and in other weatherable

543 minerals, points to a particularly ancient origin of these materials (Boelhowers, 2004). Most of the
544 morphologic features are not preserved on more easily weatherable substrates, still the analogous
545 surface shape and position indicate a similar origin and history and, thus, age, for the soils
546 developed on weatherable shales and dolomite. As the considered relict surfaces lie on an ideal
547 plane gently sloping north-eastward, following the river Tanaro downstream, the age of formation is
548 likely the same for all, even if this hypothesis will remain only speculative until some datings will
549 be available.

550 On these surfaces, strikingly different soils were developed, well associated with specific parent
551 materials, at close distance from each other. Each considered soil represents an extreme expression
552 of some features, each apparently developed under different phytoclimatic regimes.

553 However, these soils have lived through similar environmental conditions likely throughout the
554 Quaternary (or large parts of it), through the same intense pedogenetic phases during warm
555 interglacials, interrupted by much longer-lasting cryogenic disturbances during glacial periods,
556 dominated by a different suite of processes which tended to counteract the development of horizons
557 occurring during warm periods (Munroe, 2007). These processes, in fact, resulted in a strong
558 polygenesis of many of the considered relict soils.

559 However, despite the polygenesis and the similar environmental conditions to which all the soils
560 were subjected, the greatest imprintings were left by different pedogenetic process on each different
561 parent material. These specific pedogenetic processes were likely active in well characterized
562 pedogenetic environments, probably only existing during limited periods throughout their history
563 (Fig. 6). Both mineralogical composition and textural properties of the different parent lithologies
564 deeply influenced the genesis of these soils, and the preservation of specific pedogenetic features as
565 well.

566 In particular, soils developed on weatherable dolomites and Fe-rich chloritic shales tend to be
567 particularly rich in clay and Fe oxi-hydroxides, thus limiting the impact of cold periods through
568 cryoturbation. It is known, in fact, that either high clay contents or sandy textures reduce the frost
569 susceptibility of soils, by limiting the possibility of water to migrate along the freezing front and the
570 formation of ice lenses (Van Vliet-Lanoë, 1998). On less weatherable, sandy textured quartzite, the
571 fast drainage and the paucity of weatherable minerals and primary phyllosilicates created the best
572 conditions for podzolization, which apparently has been active for extremely long periods.

573 Macroscopic evidences of cryoturbation are limited to the development of localized small soil
574 wedge-casts, likely because of the sandy texture. On quartzitic substrates including also small
575 quantities of weatherable silicates (pyroxenes, feldspars, amphiboles, biotite), clay mineral
576 formation was favoured during warm interglacials, and memories of alternating warm periods

577 characterized by clay lessivage and colder ones characterized by intense podzolization are preserved
578 in the Bt and Bsm horizons respectively, and in their micromorphology. The higher silt and clay
579 content in the ORT and PLC compared with the ALB soils favoured a higher frost susceptibility, as
580 shown by the cryoturbated, dense horizons, which were likely located between the permafrost table
581 and the active layer. Soils formed on coarse and resistant to weathering quartzitic conglomerates
582 were subjected to intense podzolization, which led to the formation of ortstein horizons, and to
583 hydromorphism during particularly humid periods, evidenced by the presence of placic horizons
584 and the abundant lepidocrocite.

585

586 **6 Conclusion**

587 Soils preserved on relict surfaces in the south-western Italian Alps show signs of extremely
588 different pedogenic trends, each dominating on different lithologies, thanks to different
589 mineralogical and textural properties that induced to different weathering regimes. These soils, even
590 if dominated by single main pedogenic processes, such as podzolization, clay illuviation or
591 rubification, are characterized by strong polygenesis, with different pedogenic processes probably
592 characterizing different periods because of different climatic conditions. Even if memories of cold
593 glacial periods (i.e., cryoturbation) and of warm interglacial (i.e., clay illuviation and rubification)
594 coexist, the associations of pedogenetic phases with precise Quaternary periods is complicated, as it
595 is not possible at the moment to hypothesize a zero-point for the initiation of pedogenesis on the
596 considered relict surfaces, which would significantly contribute to the history of pedogenesis and of
597 paleo-environments during the Quaternary on the Alps, which is largely unknown. However, this
598 study represents one of the first characterization of polygenetic Quaternary paleosols on the Alpine
599 range.

600

601 **Acknowledgments**

602 This work has been funded by the POR-FESR 2007/2013 program (Poliinnovazione-Regione Piemonte).

603

604 **References**

- 605 Avila, A., Queralt-Mitjans, I., Alarcòn, M., 1997. Mineralogical composition of African dust
606 delivered by red rains over northeastern Spain. *Journal of Geophysical Research* 102(D18), 21977-
607 21996.
- 608 Bernas, B., 1968. A new method for decomposition and comprehensive analysis of silicates by
609 atomic absorption spectrometry. *Analytical Chemistry* 40, 1682-1686.

610 Biancotti, A., Bellardone, G., Bovo, S., Cagnazzi, B., Giacomelli, L., Marchisio, C., 1998.
611 Distribuzione regionale di piogge e temperature. Collana di Studi Climatologici in Piemonte,
612 Volume 1. CIMA ICAM, Torino.

613 Bloom, P.R., 2000. Soil pH and buffering. In: Sumner, M.E. (Ed.), Handbook of Soil Science. CRC
614 Press, Boca Raton, Fla, USA, pp. B333-B352.

615 Bockheim, J., 2011. Distribution and genesis of ortstein and placic horizons in soils of the USA: a
616 review. *Soil Science Society of America Journal* 75, 994–1005.

617 Boelhouwers, J., 2004. New perspectives on autochthonous blockfield development. *Polar*
618 *Geography* 28(2), 133-146.

619 Boero, V., Schwertmann, U., 1989. Iron oxide mineralogy of Terra Rossa and its genetic
620 implications. *Geoderma* 44, 319-327.

621 Bonifacio, E., Santoni, S., Celi, L., Zanini, E., 2006. Spodosol-Histosol evolution in the Krkonose
622 National Park (CZ). *Geoderma* 131, 237-250.

623 Busacca, A., Cremaschi, M., 1998. The role of time versus climate in the formation of deep soils of
624 the Apennine fringe of the Po Valley. *Quaternary International* 51/52, 95-107.

625 Buurman, P., Jongmans, A.G., Kasse, C., van Lagen, B., 1999. Discussion: oil seepage or fossil
626 podzol? An Early Oligocene oil seepage at the southern rim of the North Sea Basin, near Leuven
627 (Belgium) by E.D. van Riessen & N. Vandenberghe. *Geologie en Mijnbouw* 74: 301-312 (1996).
628 *Geologie en Mijnbouw* 77, 93-98.

629 Buurman, P., Jongmans, A.G., 2005. Podzolisation and soil organic matter dynamics. *Geoderma*
630 125, 71-83.

631 Campbell, A.S., Schwertmann, U., 1984. Iron oxide mineralogy of placic horizons. *Journal of Soil*
632 *Science* 35, 569-582.

633 Carraro, F., Giardino, M., 2004. Quaternary glaciations in the western Italian Alps: a review.
634 *Development in Quaternary Science* 2(1), 201-208.

635 Catoni, M., D'Amico, M.E., Mittelmeijer-Hazeleger, M.C., Rothenberg, G., Bonifacio, E., 2014.
636 Micropore characteristics of organic matter pools in cemented and non-cemented podzolic horizons.
637 *European Journal of Soil Science* 65, 763–773.

638 Chiang, H.C., Wang, M.K., Houg, K.H., White, N., Dixon, J., 1999. Mineralogy of B horizons in
639 alpine forest soils of Taiwan. *Soil Science* 164(2), 111-122.

640 Collins, J.F., O'Dubhain, T., 1980. A micromorphological study of silt concentrations in some Irish
641 Podzols. *Geoderma* 24:215-224.

642 Cornelis, J.T., Weis, D., Lavkulich, L., Vermeire, M.L., Delvaux, B., Barling, J., 2014. Silicon
643 isotopes record dissolution and re-precipitation of pedogenic clay minerals in a podzolic soil
644 chronosequence. *Geoderma* 235-236, 19-29.

645 Cremaschi, M., Van Vliet-Lanoë, B., 1990. Traces of frost activity and ice segregation in
646 Pleistocene loess deposits and till of northern Italy: deep seasonal freezing or permafrost?
647 *Quaternary International* 5, 39-48.

648 D'Amico, M.E., Freppaz, M., Filippa, G., Zanini, E., 2014. Vegetation influence on soil formation
649 rate in a proglacial chronosequence (Lys Glacier, NW Italian Alps). *Catena* 113, 122-137.

650 Drees, L.R., Wilding, L.P., Smeck, N.E., Senkayi, A.L., 1989. Silica in soils: quartz and disordered
651 silica polymorphs. In: Dixon JB, Weed SB (Eds.): *Minerals in Soil Environments*. Second Edition.
652 Soil Science Society of America Book Series no. 1. pp. 913-974.

653 Dubroeuq, D., Volkoff, B., 1998. From Oxisols to Spodosols and Histosols: evolution of the soil
654 mantles in the Rio Negro basin Amazonia. *Catena* 32, 245-280.

655 Durn, G., Ottner, F., Slovenec, D., 1999. Mineralogical and geochemical indicators of the
656 polygenetic nature of Terra Rossa in Istria, Croatia. *Geoderma* 91(1-2), 125-150.

657 Durn, G., 2003. Terra Rossa in the Mediterranean region: parent materials, composition and origin.
658 *Geologia Croatica* 56/1, 83-100.

659 Egli, M., Wernli, M., Kneisel, C., Haeberli, W., 2006. Melting glaciers and soil development in
660 proglacial area Morteratsch (Swiss Alps): I. Soil type chronosequence. *Arctic, Antarctic and Alpine*
661 *Research* 38(4), 499-509.

662 Falsone G., Celi L., Caimi, A., Simonov, G., Bonifacio, E., 2012. The effect of clear cutting on
663 podzolisation and soil carbon dynamics in boreal forests (Middle Taiga zone, Russia). *Geoderma*
664 177-178, 27-38.

665 FAO, 2006. *Guidelines for Soil Description*. 4th ed. FAO, Rome.

666 FAO, 2014. *World reference base for soil resources 2014*. World Soil Resources Reports 106, FAO,
667 Rome.

668 Goodfellow, B.W., 2007. Relict non-glacial surfaces in formerly glaciated landscapes. *Earth-*
669 *Science Reviews* 80 47-73.

670 Goodfellow, B.W., Stroeven, A.P., Fabel, D., Fredin, O., Derron, M.H., Bintanja, R., Caffee, M.W.,
671 2014. Arctic-alpine blockfields in northern Swedish Scandes: late Quaternary, not Neogene. *Earth*
672 *Surface Dynamics* 2, 383-401.

673 Harris, S.A., 1994. Climatic zonality of periglacial landforms in mountain areas. *Arctic* 47(2), 184-
674 192.

675 Jenny, H., Arkley, R. J., Schultz, A.M., 1969. The Pygmy forest-Podsol ecosystem and its dune
676 associates of the Mendocino Coast. *Madrono* 20, 60-74.

677 Jien, S.H., Hseu, Y., Iizuka, Y., Chen, T.H., Chiu, Y., 2010. Geochemical characterization of placic
678 horizons in subtropical montane forest soils, northeastern Taiwan. *European Journal of Soil Science*
679 61, 319-332.

680 Joerin, U.E., Stocker, T.F., Schlüchter, C., 2006. Multicentury glacier fluctuations in the Swiss Alps
681 during the Holocene. *The Holocene* 16(5), 697-704.

682 Jordanova, N., Jordanova, D., Liu, Q., Hu, P., Petrov, P., Petrovsky, E., 2013. Soil formation and
683 mineralogy of a Rhodic Luvisol - insights from magnetic and geochemical studies. *Global and*
684 *Planetary Change* 110, 397-413.

685 Kemp, R.A., 1998. Role of micromorphology in paleopedological research. *Quaternary*
686 *International* 51/52, 133-141.

687 Krauskopft, K.B., Bird, D.K., 1995. *Introduction to geochemistry*. 3rd Edition. McGraw-Hill Inc.,
688 New York, NY, USA

689 Krishnamurti, G.S.R., Huang, P.M., 1993. Formation of lepidocrocite from iron(II) solutions:
690 stabilization by citrate. *Soil Science Society of America Journal* 57(3), 861-867.

691 Lapen, D.R., Wang, C., 1999. Placic and ortstein horizon genesis and peatland development,
692 Southeastern Newfoundland. *Soil Science Society of America Journal* 63, 1472-1482.

693 Legros, J.P., 1992. Soils of the Alpine mountains. In: Martini IP, Chesworth W (eds.) *Weathering,*
694 *Soils and Paleosols*, Elsevier, Amsterdam, Netherlands, pp. 155- 181.

695 Lühti, M.P., 2014. Little Ice Age climate reconstruction from ensemble reanalysis of Alpine glacier
696 fluctuations. *The Cryosphere* 8, 639-650.

697 McKeague, J.A., DeConinck, F., Franzmeier, D.P., 1983. Spodosols. In: Smeck N.E. Hall G.F.
698 (Eds). *Pedogenesis and soil taxonomy. II: The soil orders*. Wilding L.P., Elsevier, Amsterdam,, The
699 Netherlands, pp. 217-252.

700 Mellor, A., Wilson, M.J., 1989. Origin and Significance of Gibbsite Montane Soils in Scotland,
701 U.K. *Arctic and Alpine Research* 21(4), 417-424.

702 Migoń, P., Lidmar Bergström, K., 2001. Weathering mantles and their significance for
703 geomorphological evolution of central and northern Europe since the Mesozoic. *Earth-Science*
704 *Reviews* 56, 285-324.

705 Munroe, J.S., 2007. Properties of alpine soils associated with well-developed sorted polygons in the
706 Uinta Mountains, Utah, U.S.A.. *Arctic, Antarctic and Alpine Research* 39(4), 578-591.

707 Ortu, E., Peyron, O., Bordon, A., de Beaulieu, J.L., Siniscalco, C., Caramiello, R., 2008. Lateglacial
708 and Holocene climate oscillations in the South-western Alps: An attempt at quantitative
709 reconstruction. *Quaternary International* 190(1), 71-88.

710 Priori, S., Costantini, E.A.C., Capezzuoli, E., Protano, G., Hilgers, A., Sauer, D., Sandrelli, F.,
711 2008. Pedostratigraphy of Terra Rossa and Quaternary geological evolution of a lacustrine
712 limestone plateau in central Italy. *Journal of Plant Nutrition and Soil Science* 171, 509-523.

713 Rellini, I., Trombino, L., Carbone, C., Firpo, M., 2014. Petroplinthite formation in a
714 pedosedimentary sequence along a northern Mediterranean coast: from micromorphology to
715 landscape evolution. *Journal of Soils and Sediments*, DOI: 10.1007/s11368-014-0896-2.

716 Righi, D., Van Ranst, E., De Coninck, E., Guillet, B., 1982. Microprobe study of a Placohumod in
717 the Antwerp Campine (North Belgium). *Pedologie* 23(2), 117-134

718 Righi, D., Huber, K., Keller, C., 1999. Clay formation and podzol development from postglacial
719 moraines in Switzerland. *Clay Minerals* 34, 319-332.

720 Ross, G.J., 1980. The mineralogy of Spodosols. In: Theng, B.K.G. (Eds.): *Soils with variable*
721 *charge*. Lower Hutt, New Zealand: Soil Bureau, Department of Scientific and Industrial Research,
722 pp. 127-143.

723 Ruellan, A., 1971. The history of soils: some problems of definition and interpretation. In: Yaalon,
724 D.H., Ed., *Paleopedology—Origin, Nature and Dating of Paleosols*. International Society of Soil
725 Science and Israel Universities Press, Jerusalem, Israel, pp. 3-13.

726 Sauer, D., Schüllli-Mauer, I., Sperstad, R., Sørensen, R., Stahr, K., 2009. Albeluvisol development
727 with time in loamy marine sediments of southern Norway. *Quaternary International* 209, 31-43.

728 Sauer, D., 2010. Approaches to quantify progressive soil development with time in Mediterranean
729 climate—I. Use of field criteria. *Journal of Plant Nutrition and Soil Science* 173, 822–842.

730 Schwertmann U., Taylor (1989). Iron oxides. In: Dixon JB, Weed SB (Eds): *Minerals in Soil*
731 *Environments*. Second Edition. Soil Science Society of America Book Series no. 1., pp. 379-430.

732 Stoops G., 2003. Guidelines for analysis and description of soil and regolith thin sections. Soil
733 Science Society of America. Madison, Wisconsin.

734 Targulian, V.O, Goryachkin, S.V., 2004. Soil memory: types of record, carriers, hierarchy and
735 diversity. *Revista Mexicana de Ciencias Geológicas* 21(1), 1-8

736 Thouvenin, C., Faivre, P., 1998. Les stagnosols des Alpes du Nord - Origine du blanchiment des
737 horizons minéraux superficiels Stagnosols in the northern Alps - Origin of the superficial mineral
738 layers bleaching. 16ème Congrès Mondial de Science du Sol, Montpellier, 20-26 août 1998,
739 available at: <http://natres.psu.ac.th/Link/SoilCongress/bdd/symp39/821-t.pdf>

740 Tolpeshta, I., Sokolova, T.A., Bonifacio, E., Falsone, G., 2010. Pedogenic Chlorites in Podzolic
741 Soils with Different Intensities of Hydromorphism: Origin, Properties, and Conditions of Their
742 Formation. *Eurasian Soil Science* 43, 777-787.

743 Torrent, J., Schwertmann, U., Schulze, D.G., 1980. Iron oxide mineralogy of some soils of two
744 river terrace sequences in Spain. *Geoderma* 23, 191-208.

745 Torrent, J., Schwertmann, U., Fechter, H., Alferes, F., 1983. Quantitative relationships between soil
746 color and hematite content. *Soil Science* 136(6), 354-358.

747 Tursina, T.V., 2009. Methodology for the diagnostics of soil polygenesis on the basis of macro-
748 and micromorphological studies. *Journal of Mountain Science* 6, 125-131

749 Vanossi, M., 1990. *Alpi Liguri: 11 Itinerari. Guide Geologiche Regionali. BE-MA, Pavia (Italy).*

750 van Reeuwijk, L.P., 2002. *Procedures for Soil Analysis. Technical Paper n. 9. International Soil*
751 *Reference and Information Centre. Wageningen, Netherlands.*

752 Van Vliet-Lanoë, B., 1998. Frost and soils: implications for paleosols, paleoclimates and
753 stratigraphy. *Catena* 34(1-2), 157-183.

754 Van Vliet-Lanoë, B., 2010. Frost action. In: Stoops, G., Marcelino, V., Mees, F. (Eds.),
755 *Interpretation of micromorphological features of soils and regoliths. Elsevier, Amsterdam, NL, pp.*
756 *81-108.*

757 Wilson, M.J., 1999. The origin of clay minerals in soils: past, present and future perspectives. *Clays*
758 *minerals* 34, 7-25.

759 Wilson, M.A., Righi, D., 2010. Spodic materials. In: Stoops G, Marcellino V, Mees F (Eds):
760 *Interpretation of micromorphological features of soils and regoliths. Elsevier, pp. 251-273.*

761 Yaalon, D.H., 1971. Soil-forming processes in time and space. In: Yaalon, D.H., Ed.,
762 *Paleopedology—Origin, Nature and Dating of Paleosols. International Society of Soil Science and*
763 *Israel Universities Press, Jerusalem, Israel, pp. 29–39.*

764 Yaalon, D.H., 1997. Soils in the Mediterranean region: what makes them different? *Catena* 28, 157-
765 169.

766

767 **Figure Captions**

768 Fig. 1: The study area in the Western Italian Alps (black circle). A few relict surfaces are evidenced
769 with a white line; the geographical coordinates of the sampling sites are reported in table 1.

770 Fig. 2: The studied soil profiles. From left to right: ALB (A), ORT (B), PLC (C), TR (D), ALI (E).

771 Fig. 3: X-ray spectra of air-dried (AD), ethylene glycol solvated (EG) and heated oriented mounts
772 of the E and Bs-old horizons of the ALB soil (A), of 2Bsm of the ORT and of the 2Bsm1-2Bsm2 of
773 PLC soils (B).

774 Fig. 4: X-ray spectra of orientated clay mounts from the TR and ALI 2Bt2 horizons after ethylene
775 glycol solvation (EG) and heating to 330° and 550°.

776 Fig. 5: Micromorphological features of selected horizons in ORT (4 top images, from left to right
777 2E(x), 2Eh(x), 2Bsm, 2Bt2 horizons) and PLC (bottom 2 images, 2E(x) and 2Bsm1+2Bsm2
778 horizons): a) leached albic materials; b) localized Fe and organic matter impregnation of silty
779 matrix; c) silt infillings in cracks cutting through both the groundmass and the coarse fragments; d)
780 remnants of localized clay coatings in pores; e) amorphous Fe and Al coatings with or without
781 monomorphous organic matter characteristic of spodic materials; f) clayey pedorelicts, remnants of
782 ancient disrupted clay coatings; g) laminated silt and fine sand coatings on pore walls; h) well
783 developed limpid crescentic clay coatings and infillings; i) laminated sand and silt accumulations; j)
784 laminar cracks; k) Fe cementation of the placic horizon.

785 Fig. 6: graphical summary of the main paleo-environmental memories imprinted in the considered
786 relicts soils.

Table 1: Site location, main environmental parameters and soil classification.

Profile code	Location	Coordinates	Substrate / parent material	Geological formation	Slope angle	Elevation (m a.s.l.)	Forest vegetation	Classification (FAO, 2014)
ALB	Toria - Pian del Pino	44°08'51.29"; 7°47'37.81"	Quartzite	Quarziti di Ponte di Nava	1	1595	<i>Pinus uncinata</i> Mill.	Albic Dystric Arenosol (Protospodic)
ORT	Pornassino - Pian degli Uccelli	44°08'18.17"; 7°48'32.40"	Quartzite - Andesite conglomerate	Porfidi di Osiglia	2	1395	<i>Pinus sylvestris</i> L.	Ortsteinic Albic Skeletic Podzol (Loamic, Hyperspodic)
PLC	Colma di Casotto	44°13'09.01"; 7°56'56.67"	Quartzitic conglomerate	Porfiroidi del Melogno	5	1445	<i>Fagus sylvatica</i> L.	Albic Ortsteinic Skeletic Podzol (Loamic Placic)
TR	Bagnasco	44°14'42.82"; 8°00'54.98"	Dolomite	Dolomie di San Pietro dei Monti	5	950	<i>Ostrya carpinifolia</i> Scop.	Rhodic Luvisol (Clayic, Cutanic)
ALI	Priola	44°17'00.72"; 8°02'31.06"	Chlorite-rich shale	Formazione di Murialdo - Scisti di Viola	10	680	<i>Castanea sativa</i> Mill. - <i>Pinus sylvestris</i> L.	Rhodic Alisol (Clayic, Hyperallic)

Table 2: main morphological properties of selected soil horizons. The set of described properties depend on the type of soil and horizon and, where not specified, the classification follows the guidelines reported by FAO 2006.

Profile	Horizon	Lower boundary ¹	Colours (mottle colors, %) ²	Structure	Consistence	Rock Fragments	Siltcaps	Frost wedges	Clay cutans	Mn-Fe cutans
		cm	Munsell, humid	Shape ³ , dimension-degree	Class ⁴	%, weathering degree ⁵	% stones covered, thickness (mm)	Width*depth (cm)	Class of abundance ⁶	Class of abundance ⁶
ALB	Oi+Oe+Oa	11		M		0				
	AE1	21/23	10YR 4/2	SG	L	20,LA				
	AE2	35	10YR 5/2	SB, ME-WE	L	20,LA		10*50		
	2EA	50	10YR 6/2	SB, ME-WE	L	40,AA		10*50		
	2E	100	10YR 7/1	SB, ME-WE	L	80,AA				
	2EB(s)	210+	7.5YR 6/3	SB, CO-MO	FR	70,AA				
	Bs-old	n.d.	7.5YR7/8 10YR 5/4	SB, CO-ST	CR	80,LA				
	Bs-young	n.d.	7.5YR 5/6	SB, ME-WE	CR	80,LA				
ORT	Oi+Oa	10		M	L					
	E	45/60	10YR 5/3	SG	FR	50,LA	5,0.3			
	2E(x)	80/95	10YR 5/3 10YR 6/3 10YR 7/4	SB, ME-ST	CP	20,AA	10,0.3			
	2Eh(x)	115/140	10YR 7/4 10YR 5/3	PL, VC-ST	CP	20,AA	10,0.3			
	2Eh	120/140*	10YR 4/2	SG	FR	20,AA				
	2Btm(s)	140*	5YR 5/6	PL, VC-ST	C	5,AA			F	
	2Bsm	180/200	7.5YR 5/6	PL, VC-WE	CC	30,AA				
	2Btsm	220/230	5YR 5/8	SB, CO-WE	CC	30,AA			C	
	2Bshm	270	7.5YR 4/6	SB, CO-WE	CC	50,LA				

			7.5YR 3/3						
	R/Cm/Cr	(Cm) 320	7.5YR 7/3	Massive	C	50,AA			
		(Cr) 350	GLE Y1-8/5GY (7.5YR 6/8, 10%)	PL-R	CP	AA			
PLC	Oi+Oa	4		M					
	A	14/4	2.5Y 3/1	SB, ME-MO, GR, FI-MO	FR	50,LA			
	AE	26	2.5Y 3/2	SB, ME-MO, GR, FI-MO	L	50,LA			
	2EA	44/42	2.5Y 6/2	SB, ME-MO, GR, FI-MO	FR	50,AA	100,3		
	2E(x)	62/67	10YR 10/2 (GLE Y1 7/3, 10%)		CP	50,AA	100,10		
	2Bsm1 (placic)	62.5/67.5	7.5YR 2/2 7.5YR 4/6		CC				
	2Bsm2	69/77	7.5YR 5/6		C	80,LA			
	2Bsm3	103+	10YR 6/8		C	80,LA			
TR	A	2/10	5YR 3/3	GR, CO-ST	L	20,LA			
	BA	53	5YR 4/6	AB, FI-ST	FR	0		F	
	Bt1	120	2.5YR 4/8	AB, VC-MO AB, FI-ST	FR	0		D	C
	Bt2	151/160	2.5YR 4/8	AB, CO-ST SN, ME-ST	FR	2,MA		A	F
	BC	170	2.5YR 4/8 10YR 5/2	PL, CO-WE	CP	20,MA		F	
	Cr	180+				99,MA			
ALI	A/Oe	1/5		GR, FI-ST	L	0			
	A	7	7.5YR 4/4	GR, VF-MO	L	10,AA			
	AB	32/40	5YR 5/8	GR, FI-MO, SB, ME-MO	FR	10,AA			

	2Bt1	50/55	2.5YR 4/6	AB, FI-ST	FR	20,AA			F	F
	2Bt2	125+	2.5YR 4/6	AB, VC-ST	M	3,AA			D	C
	2BC		2.5YR 5/8	PL-R	M	90,MA			A	

¹ discontinuous horizons are indicated with *;

² all the colours detected in the horizon; the colours in brackets represent mottles caused by waterlogging;

³ Shape: M: matted; SG: single grain; SB: subangular blocky; PL: platy; GR: biogenic granular aggregates; AB: blocky polyhedral; PL-R: platy, weathered rock structure. Dimension: VF: very fine; FI: fine; ME: medium; CO: coarse; VC: very coarse. Degree: VE: weak; MO: moderate; ST: strong.

⁴ Consistence: L: loose; FR: friable; CR: crumby; CP: compacted; C: weakly cemented; CC: strongly cemented;

⁵ Rock fragments weathering degree: LA: fresh; AA: moderately weathered; MA: strongly weathered, soft.

⁶ Abundance class: F: few; C: common; A: abundant; D: dominant

Table 3: main chemical properties of the mineral soil horizons

Name	Horizon	pH H ₂ O	pH NaF	CaCO ₃	C org	CEC ¹	BS ¹	Sand	Silt	Clay
				g kg ⁻¹	g kg ⁻¹	cmol _c kg ⁻¹	%	%	%	%
ALB	AE1	3.4	7.5		34.1			76.3	13.5	10.2
	AE2	3.9	7.5		5.5					
	2EA	4.3	7.5		1.5			79.7	12.8	7.5
	2E	4.8	7.5		0.0			80.1	14.0	5.9
	2EB(s)	4.3	7.5		2.1			77.3	14.9	7.9
	Bs-old	5.1	9.0					48.5	32.9	18.6
	Bs-young	5.1	12.5		21.2			63.7	16.1	20.2
ORT	2E(x)	4.8	7.8		1.0			79.3	11.9	8.9
	2Eh(x)	4.4	8.0		4.3			74.6	13.7	11.7
	2Eh	4.5	7.5		2.4					
	2Btm(s)	5.0	8.8		1.3			78.6	5.1	16.3
	2Bsm	5.2	11.0		3.3			74.7	12.9	12.4
	2Btsm	5.2	10.0		2.3			65.4	11.6	23.0
	2Bshm	5.0	11.8		3.8			66.2	14.4	19.4
PLC	A	3.8	7.5		39.1			64.0	18.4	17.6
	AE	3.9	7.5		24.1			66.0	16.0	18.0
	2EA	3.9	7.5		6.3			64.3	23.4	12.3
	2E(x)	4.3	7.5		2.9			67.0	23.9	9.1
	2Bsm1+2Bsm2	4.6	8.5		2.2			69.5	22.3	8.2
	2Bsm3	4.7	8.2		0.9			57.4	33.9	8.7
TR	A	7.0		3.1	30.4	31.5	86.5	10.3	24.6	65.1
	BA	7.1		2.5	9.5	25.8	84.3	16.7	22.4	60.8
	Bt1	7.3		1.6	4.0	19.7	94.4	8.4	18.2	73.5
	Bt2	7.4		3.6		24.4	100.0	16.4	15.3	68.3
	Cr	8.1		104.9		7.6	100.0	31.6	32.2	36.1
ALI	AB	4.4	8.3		10.1	31.0	2.8	27.2	29.2	43.6
	2Bt1	4.7	8.5		4.4	30.7	4.3	11.5	35.6	52.9
	2Bt2	4.9	8.5		1.4	30.4	7.2	10.9	32.4	56.7
	2CB	4.7	8.3		2.2	15.6	6.4	43.3	25.8	31.0

¹CEC: Cation Exchange Capacity, BS: base saturation

Table 4: Fe, Al and Si total contents and fractionation

Profile	Horizon	Fe _o	Al _o	ISP	Fe _d	Fe _o /Fe _d	Fe _t	Al _t	Si _t	Fe _d /Fe _t
		g kg ⁻¹	g kg ⁻¹	%	g kg ⁻¹		g kg ⁻¹	g kg ⁻¹	g kg ⁻¹	
ALB	AE1	0.27	0.27	0.04	1.04	0.26	2.4	11.9	412.5	0.43
	AE2	0.09	0.11	0.02	0.44	0.21	2.2	11.8	435.1	0.20
	2EA	0.04	0.09	0.01	0.36	0.11	1.8	10.3	447.1	0.20
	2E	0.03	0.07	0.01	0.18	0.15	3.3	7.5	450.6	0.05
	2EB(s)	0.08	0.21	0.03	0.12	0.68	3.0	21.8	436.7	0.04
	Bs-old	1.67	1.46	0.23	3.61	0.46				
	Bs-young	5.52	5.63	0.84	8.09	0.68	15.5	41.7	403.9	0.52
	Parent rock						6.3	27.4	409.9	
ORT	2E(x)	0.53	0.42	0.07	1.04	0.51	4.3	15.0	439.4	0.24
	2Eh(x)	1.17	0.76	0.13	3.36	0.35	7.1	21.3	426.8	0.47
	2Eh	1.04	0.68	0.12	2.28	0.46	5.2	17.0	433.9	0.44
	2Btm(s)	0.86	1.29	0.17	6.05	0.14	22.9	77.8	344.7	0.26
	2Bsm	1.45	2.97	0.37	6.78	0.21	93.9	126.2	250.9	0.07
	2Btsm	1.04	2.90	0.34	8.67	0.12	15.7	34.2	396.4	0.55
	2Bshm	2.02	2.40	0.34	5.50	0.37	12.4	33.4	405.4	0.44
	CBm	0.14	0.18	0.03	0.46	0.30	3.3	23.2	438.1	0.14
	Cr	0.23	0.28	0.04	1.15	0.20	22.4	105.6	316.6	0.05
	Parent rock						13.5	22.7	415.6	
PLC	A	1.64	2.12	0.29	4.16	0.39	19.1	37.8	348.1	0.22
	AE	0.95	1.31	0.18	2.40	0.40	16.0	34.7	375.5	0.15
	2EA	0.43	0.68	0.09	1.06	0.40	13.5	28.4	398.5	0.08
	2E(x)	0.20	0.50	0.06	0.65	0.31	13.3	27.6	400.7	0.05
	2Bsm1+2Bsm2	3.17	0.76	0.23	4.57	0.69	20.7	36.9	385.9	0.22
	2Bsm3	2.98	0.77	0.23	4.26	0.70	18.2	37.4	388.9	0.23
TR	A	1.50	2.24	0.30	37.18	0.04	75.9	100.8	195.1	0.49
	BA	1.34	1.59	0.23	42.30	0.03	91.3	103.9	207.8	0.46
	Bt1	1.31	1.58	0.22	43.33	0.03	83.0	110.3	201.0	0.52
	Bt2	1.42	1.35	0.21	44.56	0.03	77.7	89.9	180.9	0.57
	Cr	0.17	0.66	0.07	10.68	0.02	18.6	21.8	45.6	0.57
ALI	AB	1.44	1.44	0.22	34.73	0.04	61.2	115.6	260.7	0.57
	2Bt1	2.03	1.42	0.24	37.64	0.05	60.9	94.6	282.2	0.62
	2Bt2	1.92	1.21	0.22	34.58	0.06	53.0	120.2	269.8	0.65
	2CB	1.90	0.90	0.19		0.05	28.2	122.8	277.5	
	Parent rock						30.1	126.8	295.0	

Table 5: Micromorphological features of selected soil horizons.

Profile	Horizon	Coarse fragments	Primary voids	Secondary voids	Cf-related distribution	b-fabric	Clay coatings	Amorphous OM-metal coatings	Organic matter coatings	Silt accumulation features	Pedorelicts
		%	(%, type)	(%, type)			%	%	%	(%, location)	(%, type)
ORT	2E(x)	70	2, vughs	1, cracks	Close porphyric	Striated	0.2	0.2	1	1	0.1
	2Eh(x)	60	2, vughs	2, cracks	Close porphyric		0.1	0.3	1	2	0.1
	2Bsm	40	30, compound packing voids	5, cracks	Close porphyric		0.2	8	0.1	2	1
	2Bt _{sm}	40	7, vughs, compound packing voids	3, cracks	Close porphyric / Chitonic	Striated	6.5	1	0.4	2	0.2
PLC	2E(x)	40	15, planes	5, cracks	Close porphyric	Striated	0.5	0.1	0.2	2	0.2
	2B _{sm1}	40	5, cracks		Double-spaced - open porphyric	Undifferentiated	0.1		0.2	1.5	0.1
	2B _{sm2}	40	30, compound packing voids		Gefuric			2	0.2		0.2

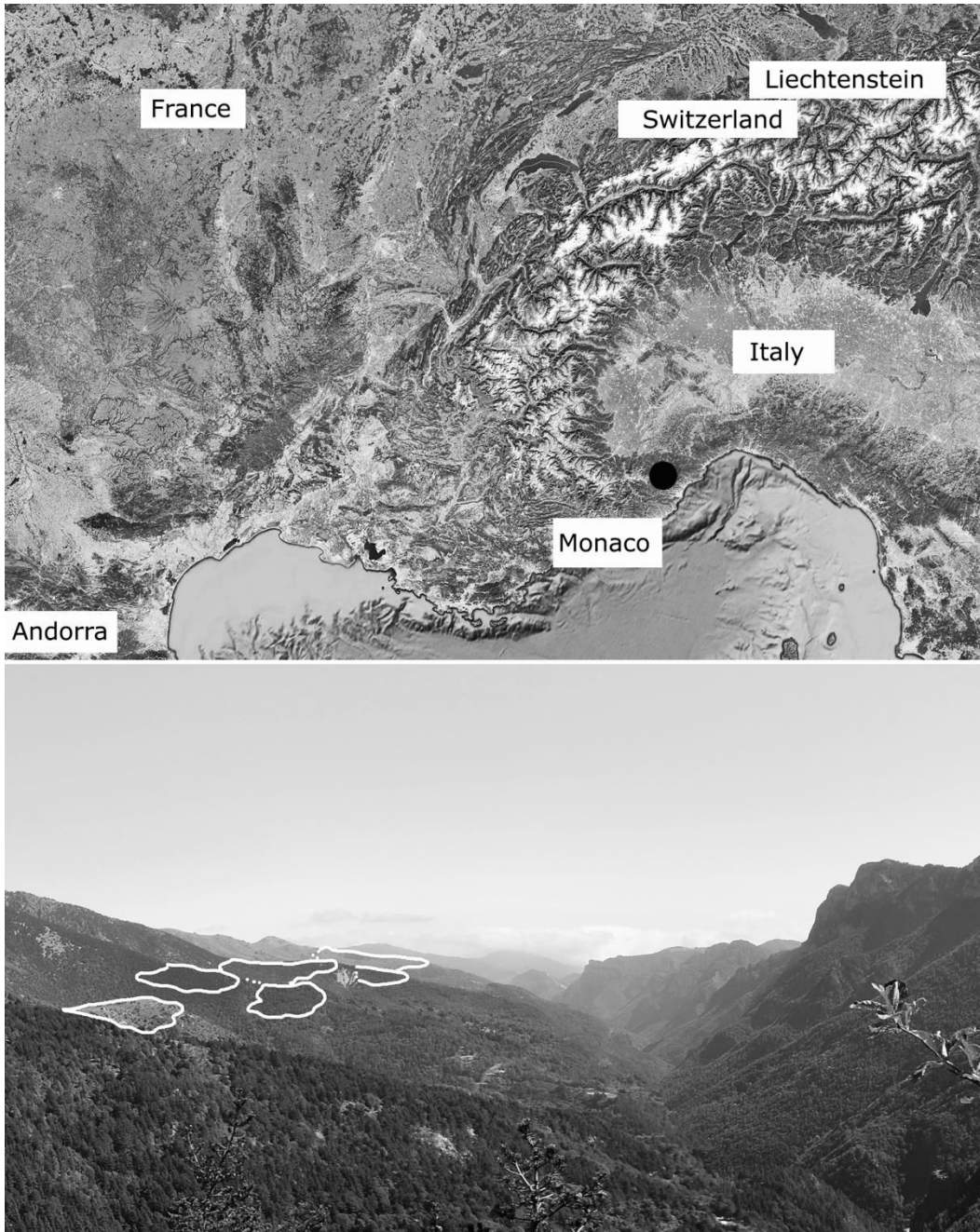


Fig. 1: The study area in the Western Italian Alps (black circle). A few relict surfaces are evidenced with a white line; the geographical coordinates of the sampling sites are reported in table 1.

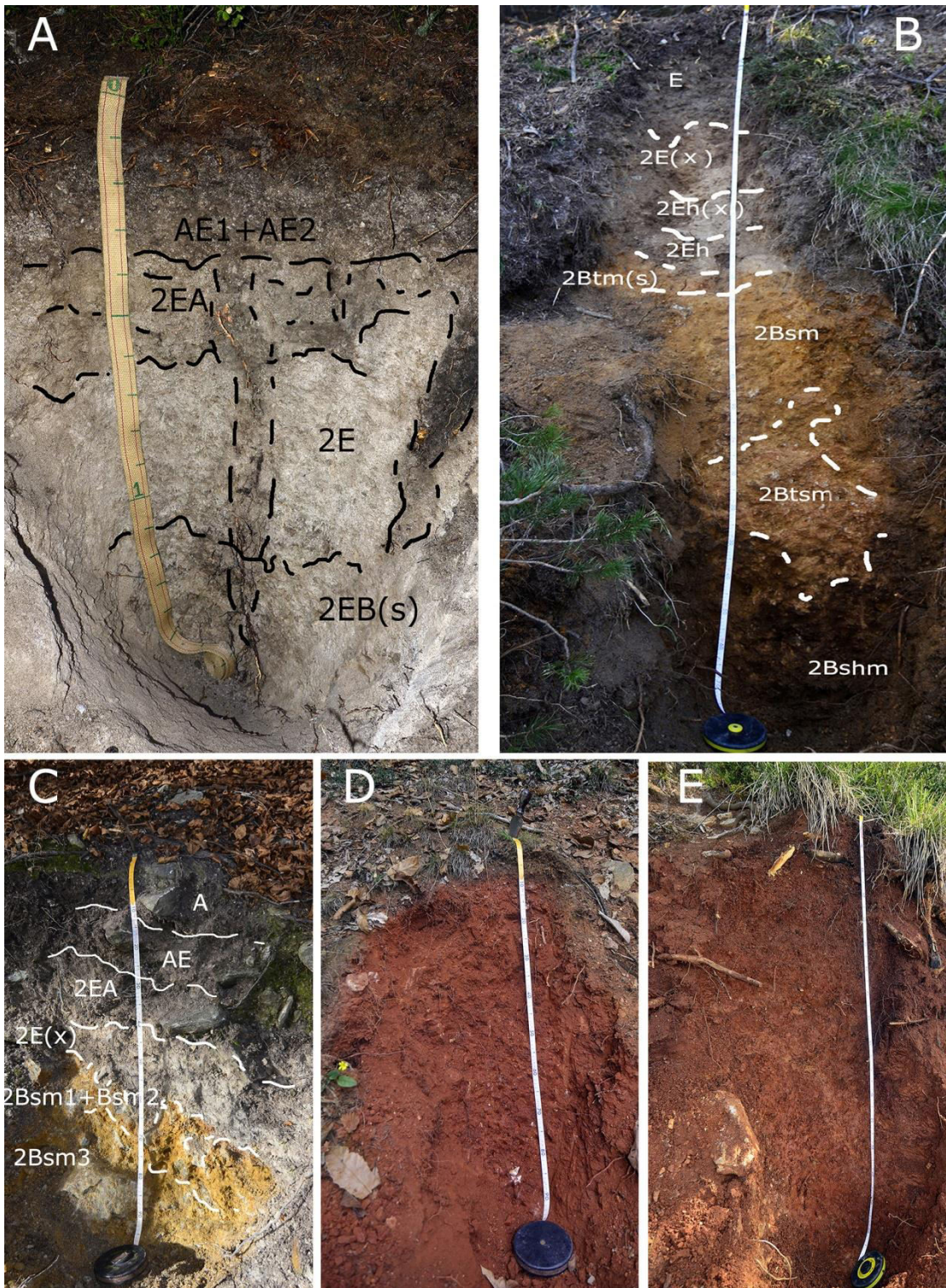


Fig. 2: The studied soil profiles. From left to right: ALB (A), ORT (B), PLC (C), TR (D), ALI (E).

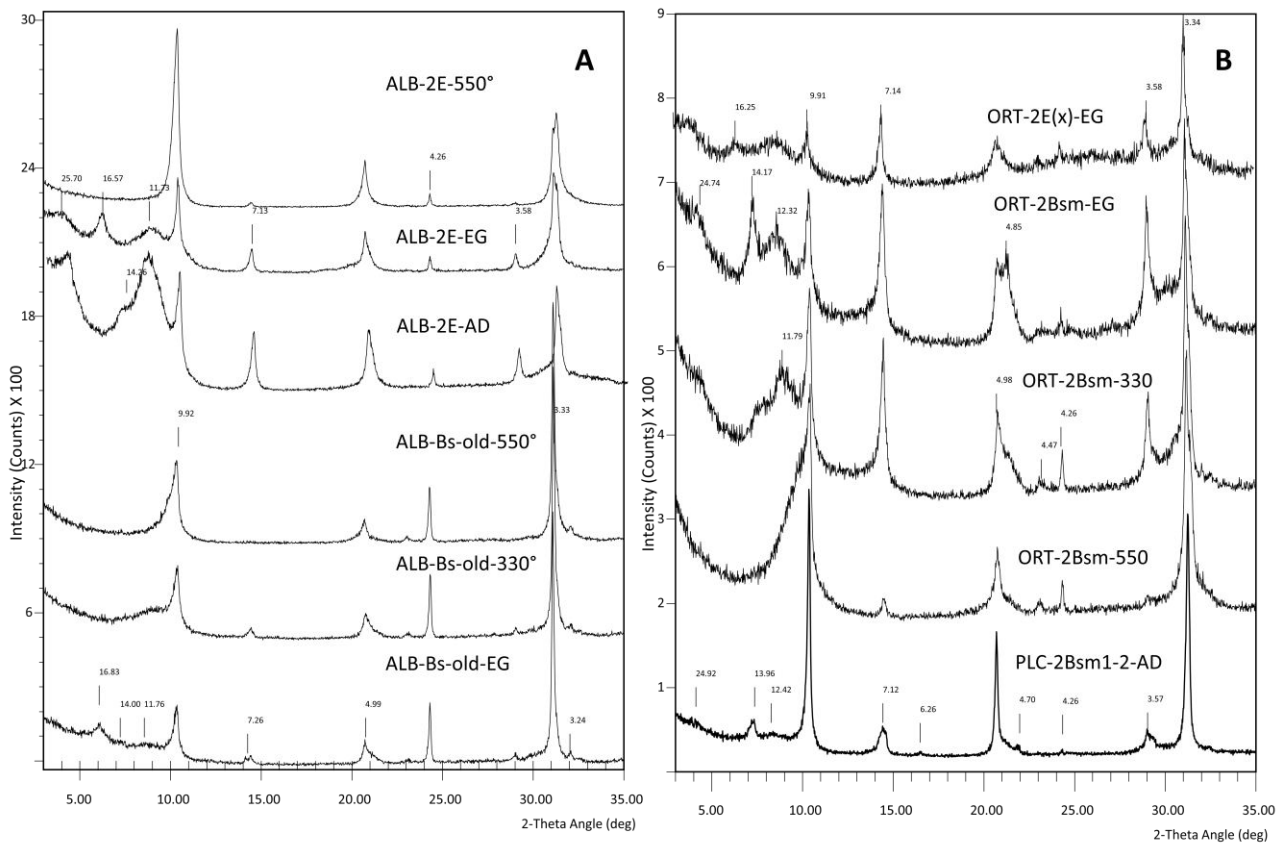


Fig. 3: X-ray spectra of air-dried (AD), ethylene glycol solvated (EG) and heated oriented mounts of the E and Bs-old horizons of the ALB soil (A), of 2Bsm of the ORT and of the 2Bsm1-2Bsm2 of PLC soils (B).

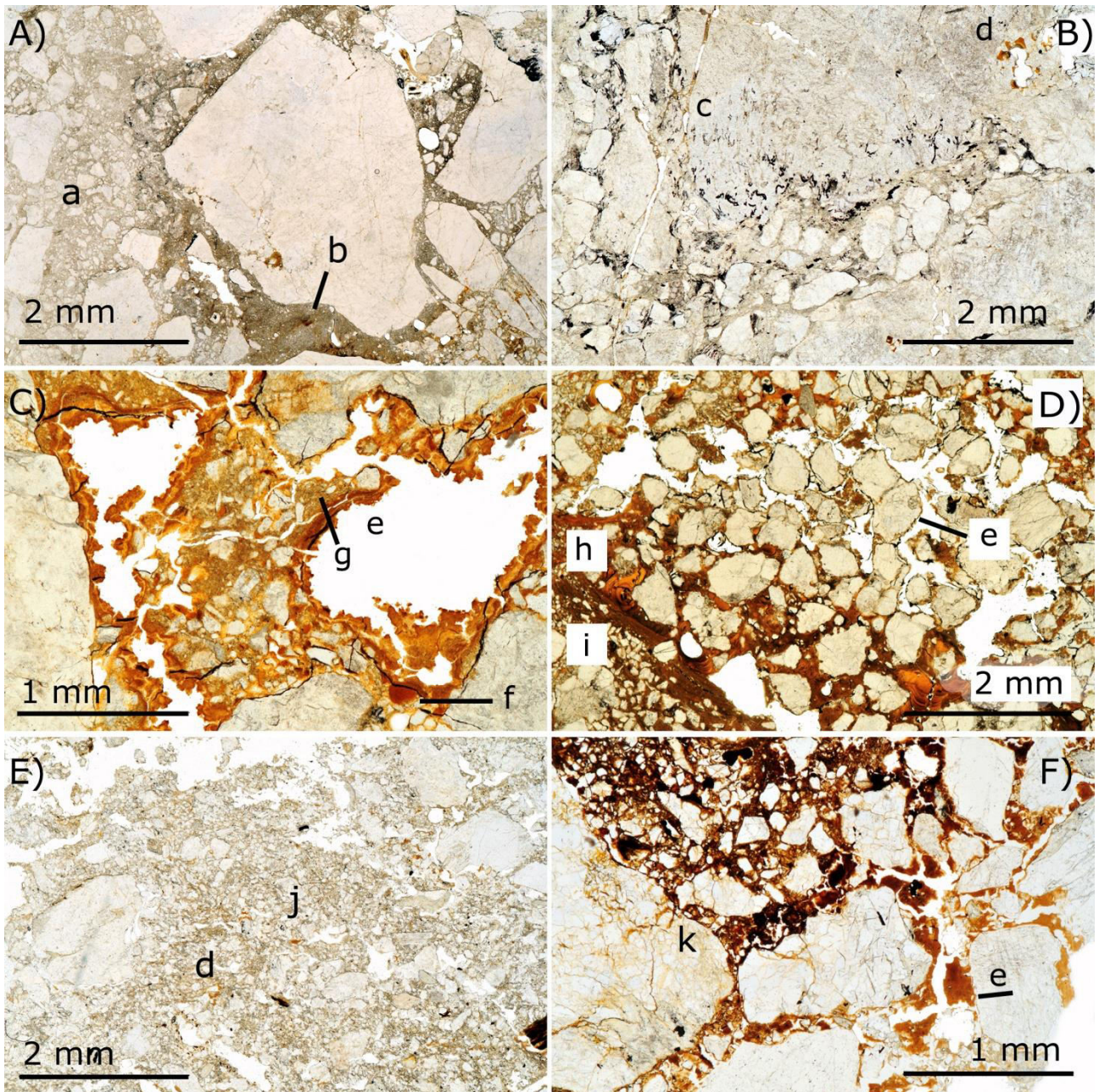


Fig. 4: Micromorphological features of selected horizons in ORT (fig. 4A, 4B, 4C, 4D, corresponding to 2E(x), 2Eh(x), 2Bsm, 2Btsm horizons respectively) and PLC (fig. 4E, 4F, corresponding to 2E(x) and 2Bsm1+2Bsm2 horizons). Some micromorphological features are visible: a) leached albic materials; b) localized Fe and organic matter impregnation of silty matrix; c) silt infillings in cracks cutting through both the groundmass and the coarse fragments; d) remnants of localized clay coatings in pores; e) amorphous Fe and Al coatings with or without monomorphic organic matter characteristic of spodic materials; f) clayey pedorelicts, remnants of ancient disrupted clay coatings; g) laminated silt and fine sand coatings on pore walls; h) well developed limpid crescentic clay coatings and infillings; i) laminated sand and silt accumulations; j) laminar cracks; k) Fe cementation of the placic horizon.

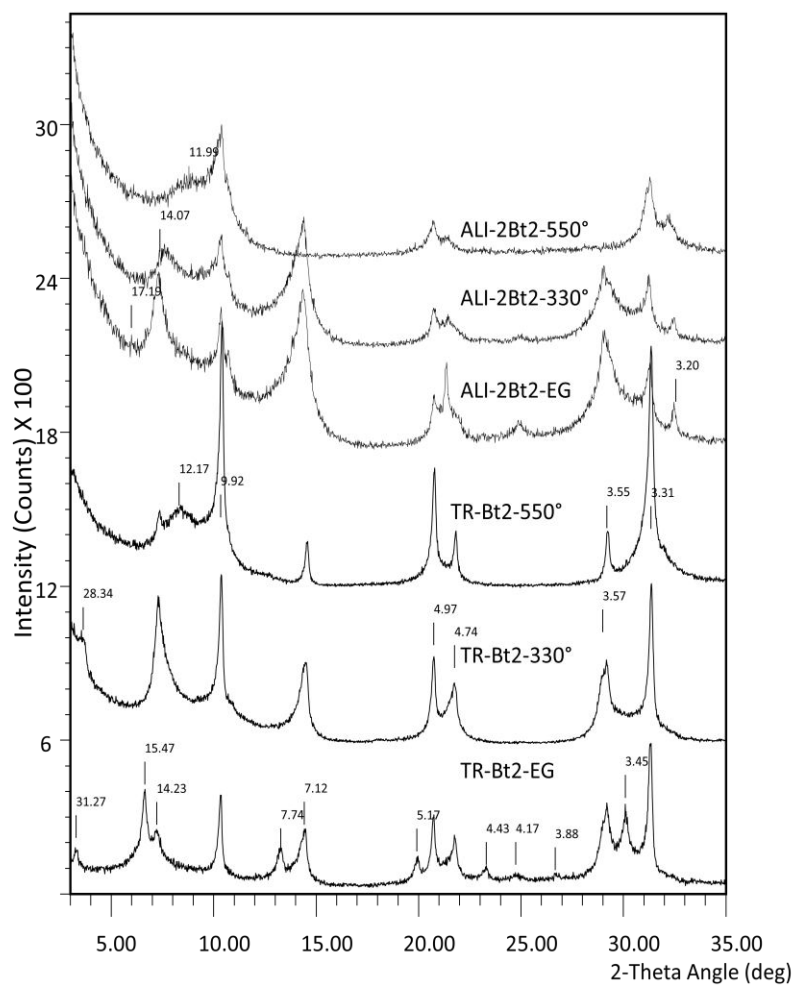


Fig. 5: X-ray spectra of orientated clay mounts from the TR and ALI 2Bt2 horizons after ethylene glycol solvation (EG) and heating to 330° and 550°.

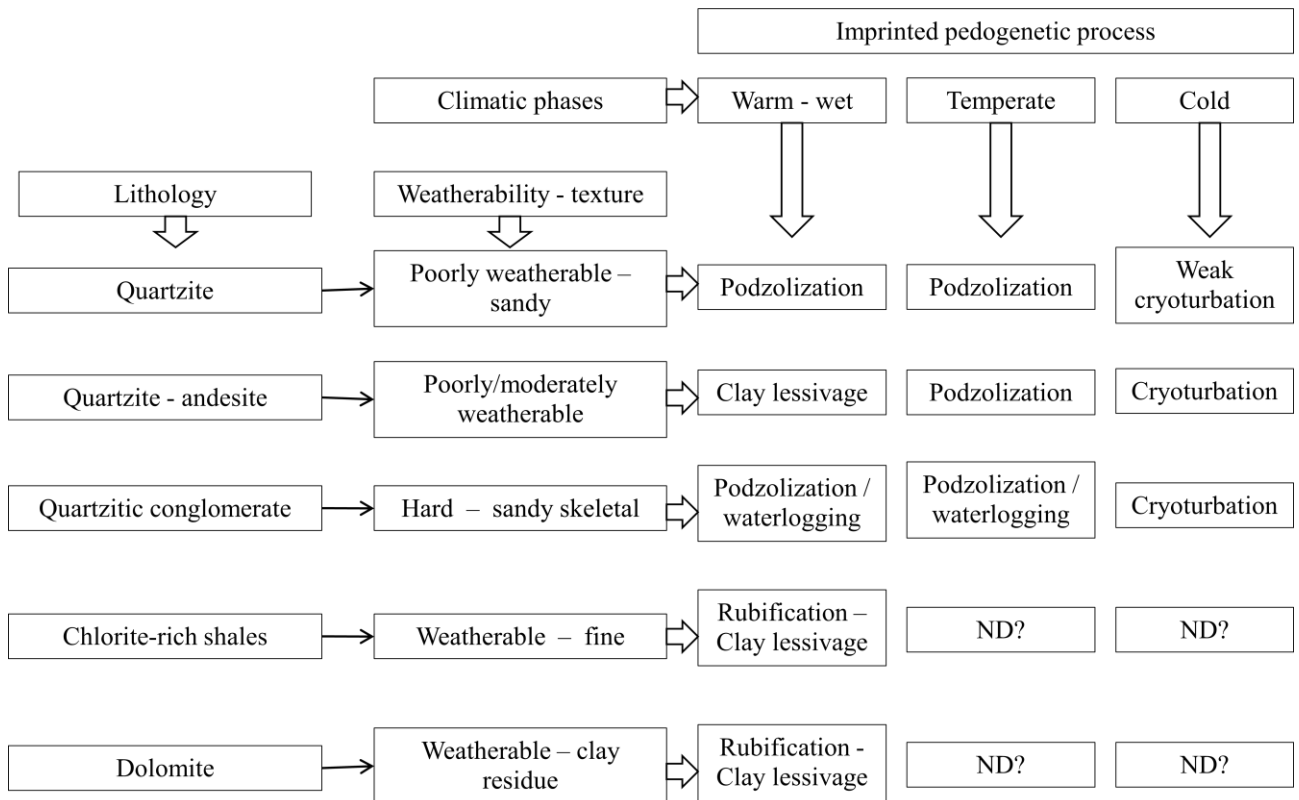


Fig. 6: graphical summary of the main paleo-environmental memories imprinted in the considered relicts soils.